Journal of Physiology (1993), **462**, *pp.* 321–347
With 13 *figures*
Printed in Great Britain

PHOTO-RELEASED INTRACELLULAR Ca^{2+} RAPIDLY BLOCKS Ba^{2+} CURRENT IN *LYMNAEA* NEURONS

BY BARRY D. JOHNSON AND LOU BYERLY*

From the Department of Biological Sciences, University of Southern California, Los Angeles, CA 90089-2520, USA

(*Received 7 April 1992*)

SUMMARY

1. The effect of intracellular Ca^{2+} on Ba^{2+} current flowing through voltage-dependent Ca^{2+} channels was studied using the whole-cell patch-clamp technique on isolated neurons from the snail *Lymnaea stagnalis*. Intracellular Ca^{2+} was increased by flash photolysis of the caged Ca^{2+} compound DM-nitrophen and measured with the optical indicator fluo-3.

2. After the highest intensity flashes, peak Ba^{2+} current was blocked by 42% with a time constant of 5 ms. The onset of the block followed a similar time course whether channels were activated or closed. The Ba^{2+} current surviving after the flash had the same voltage dependence of activation and rate of inactivation as did the total Ba^{2+} current before the flash.

3. Recovery of the Ba^{2+} current from block was nearly complete and occurred with a time constant of 16 s. Multiple episodes of photolysis-induced block could be studied in the same cell when 7–10 min were allowed between flashes. In some cells, recovery from block was accompanied by a transient enhancement of the current above the pre-block magnitude.

4. Neurons greatly reduced the ability of photolysis to increase Ca^{2+}, both by unloading the DM-nitrophen before flashes were applied and by rapidly buffering the photolytically released Ca^{2+}. Maximal flashes on extracellular droplets of the DM–Ca^{2+} solution created a Ca^{2+} jump from 110 nM to 40 μM. In contrast, the same flashes on DM–Ca^{2+}-loaded neurons resulted in a Ca^{2+} transient starting from a baseline of 36 nM to a peak of 130 nM. This intracellular Ca^{2+} transient decayed with three time constants (120 ms, 2 s and 13 s).

5. Endogenous buffer(s) binds Ca^{2+} rapidly. When intracellular Ca^{2+} was monitored within 2 ms of the flash, no rapid Ca^{2+} spike due to binding of photo-released Ca^{2+} could be detected. Addition of dibromo-BAPTA to the intracellular solution reduced the block by one third, which is consistent with the measured reduction of intracellular Ca^{2+}. This indicates that the endogenous buffer can bind Ca^{2+} as rapidly as dibromo-BAPTA and as fast as Ca^{2+} is released by photolysis.

6. The Ca^{2+} dependence of the block, obtained by varying flash intensity, indicates some saturation by 130 nM. A simple two-state model of the block consistent with

* To whom reprint requests should be sent.

MS 1267

both the time course of block and recovery and the concentration dependence gave a dissociation constant of ≈ 50 nM and forward rate constant of 7×10^8 M^{-1} s^{-1}.

7. These results indicate that *Lymnaea* Ca^{2+} channels are blocked by Ca^{2+} in the submicromolar range at a rate near the diffusion limit. The speed of the block requires a very simple mechanism, perhaps direct binding to the channel macromolecule. These experiments also demonstrate that neuronal Ca^{2+} buffering is strong and rapid. Direct measurement of intracellular Ca^{2+} is essential if photolysis experiments are to be interpreted quantitatively.

INTRODUCTION

The suggestion that intracellular Ca^{2+} blocks Ca^{2+} channels emerged from Hagiwara & Nakajima's (1966) discovery that the Ca^{2+} spike of barnacle muscle was blocked by intracellular Ca^{2+} higher than 1 μM. Experiments in *Paramecium* (Brehm & Eckert, 1978) and *Aplysia* neurons (Tillotson, 1979) supported this role for intracellular Ca^{2+}, demonstrating that Ca^{2+} channel inactivation was related to the influx of Ca^{2+}. Following those initial studies, Ca^{2+}-dependent inactivation of Ca^{2+} currents has been demonstrated in many cells throughout the animal kingdom (Eckert & Chad, 1984). A primary goal of the study we present here is to determine the range of intracellular Ca^{2+} concentrations that block Ca^{2+} channels.

Although previous studies on snail neuron Ca^{2+} currents indicated a submicromolar Ca^{2+} sensitivity, interpretation of these experiments is limited due to the inability to uniformly alter intracellular Ca^{2+}. By direct injection of buffered Ca^{2+} solutions, Plant, Standen & Ward (1983) were able to show that the Ca^{2+} current of *Helix* neurons was sensitive to intracellular Ca^{2+} in the submicromolar range (0·1–1 μM). Internal dialysis of snail neurons using large-opening suction electrodes appeared to offer a method of changing intracellular Ca^{2+} more homogeneously than injection. Kostyuk & Krishtal (1977) found that 60 nM Ca^{2+} completely and reversibly blocked Ca^{2+} current in *Helix* neurons. However, Byerly & Moody (1984) showed that intracellular Ca^{2+} (measured with a Ca^{2+}-sensitive microelectrode) was not reliably controlled by dialysis with the electrode solution. Intracellular Ca^{2+} could be increased rapidly only after ATP was omitted from the dialysis solution. Unfortunately, the absence of ATP caused unstable Ca^{2+} current which declined ('washed out') in spite of the buffered low-Ca^{2+} electrode solutions used. Ca^{2+} currents were 'blocked' by intracellular Ca^{2+} at concentrations less than 1 μM, and this block could be reversed if the cell was immediately dialysed with a low-Ca^{2+}, ATP-containing solution (Byerly, Leung & Yazejian, 1988); however, it was not clear if Ca^{2+} current block was due to the increase of intracellular Ca^{2+} or to the depletion of ATP.

The submicromolar Ca^{2+} sensitivity of Ca^{2+} currents suggested by the above and other studies does not seem consistent with the low sensitivity to intracellular Ca^{2+} suggested by experiments on Ca^{2+} channels in bilayers, or by recent models for Ca^{2+}-dependent inactivation of Ca^{2+} channels. Cardiac Ca^{2+} channels, which show Ca^{2+}-dependent inactivation in whole-cell recordings (Lee, Marban & Tsien, 1985), are only blocked by millimolar Ca^{2+} ($K_d = 4$ mM) on the intracellular side of planar lipid bilayers (Rosenberg, Hess & Tsien, 1988). Smooth muscle Ca^{2+} channels studied in bilayers also show a low sensitivity to intracellular Ca^{2+} (Huang, Quale, Worley,

Standen & Nelson, 1989). Simple biophysical models predict that Ca^{2+} at the inner mouth of the Ca^{2+} channel should reach millimolar levels within microseconds of channel opening (Simon & Llinás, 1985; Neher, 1986). Assuming a Ca^{2+} binding site at the inner mouth of pancreatic β-cell Ca^{2+} channels, Sherman, Keizer & Rinzel (1990) proposed a model for Ca^{2+}-dependent inactivation using a dissociation constant of 0·5 mM. These widely different sensitivities to intracellular Ca^{2+} may be due to different experimental conditions, inherent differences between types of Ca^{2+} channels, or the presence of more than one site at which Ca^{2+} binding reduces Ca^{2+} channel function.

The most significant limitation on whole-cell studies of Ca^{2+} channel block by intracellular Ca^{2+} has been the control over intracellular Ca^{2+}. The relatively new technique of Ca^{2+} photo-release from 'caged' compounds provides a method for rapidly raising intracellular Ca^{2+} in a uniform manner, without changing other intracellular metabolites such as ATP. This allows a direct and quantitative test of intracellular Ca^{2+} action on Ca^{2+} currents. Flash photolysis of the 'caged' Ca^{2+} ligand, DM-nitrophen, in dorsal root ganglion neurons was found to block Ca^{2+} current with a time constant of 7 ms (Morad, Davies, Kaplan & Lux, 1988). However, the blocking concentration of intracellular Ca^{2+} was not measured in those experiments. In the present study, we have applied flash photolysis of DM-nitrophen to the Ba^{2+} current of isolated snail neurons and have measured the levels of intracellular Ca^{2+} with fluo-3. The fluo-3 measurements indicate that jumps of Ca^{2+} inside the dialysed neurons are much smaller than those obtained by flashing droplets of the same solution outside the cell. Apparently the dialysed cell cytoplasm strongly and rapidly buffers Ca^{2+}. Flashes that jump intracellular Ca^{2+} to 130 nM rapidly block (time constant, $\tau = 5$ ms) about half of the Ba^{2+} current present at the steady-state Ca^{2+} level (36 nM). Ba^{2+} current recovers from block with a time constant of 16 s. A simple two-state model with a K_d of 50 nM fits the data reasonably well. Preliminary reports on this research have been published (Johnson & Byerly, 1991*a*, *b*).

METHODS

Cell preparation and electrophysiology

Pedal, parietal, and visceral ganglia from the freshwater snail *Lymnaea stagnalis* were treated for 20 min at 29 °C in protease (Sigma Type XIV, 1 mg ml^{-1}) and for 1 h at 29 °C in trypsin (Sigma Type III, 2 mg ml^{-1}), desheathed, and then dissociated in glucose-containing *Lymnaea* saline. Isolated neurons were allowed at least 1 h to recover and to reabsorb axons. The nearly spherical cell bodies were studied at room temperature (23 °C) either the day of isolation or refrigerated overnight (16 h, 5 °C) and used the following day. Individual neurons (40–60 μm) were transferred into the recording chamber and patch clamped in the whole-cell configuration, using a Dagan 8900 amplifier. Whole-cell seals were between 100 MΩ and 1 GΩ. Patch electrodes were double pulled (Narishige PP-83 puller) from 100 μl pipette glass (VWR) to produce a tip diameter of 8–12 μm. These electrodes were painted with a heavy black paint to within 100 μm of the tip and then fire-polished to a tip diameter of 7–10 μm. The purpose of the black paint was to minimize the photolysis of DM-nitrophen in the patch electrode. Data were acquired and analysed using a Labmaster interface and pCLAMP software (Axon Instruments). Graphics and statistics were generated with SYSTAT (Systat, Inc.) and Freelance (Lotus) software packages.

Ba^{2+} current was isolated from other membrane currents by the following procedure. K^+ and Na^+ currents were eliminated by replacing all K^+ and Na^+ with impermeable ions (see *Solutions*). Linear leak current was measured as the sum of the currents from four hyperpolarizing steps of one-fourth the magnitude of the test potential (P/4 paradigm) and subtracted from the current recorded at the test potential. Proton current was measured at the end of each experiment after external

application of 10 mM tetrapentylammonium (TPeA; Augustine, Charlton & Horn, 1988) and then subtracted from all the 'Ba^{2+}-currents' measured during the experiment. TPeA irreversibly blocks all voltage-dependent currents (Na^+, K^+, Ca^{2+}) except proton currents (Byerly & Suen, 1989; B. Johnson, unpublished results). The possible contribution of proton current to current recordings

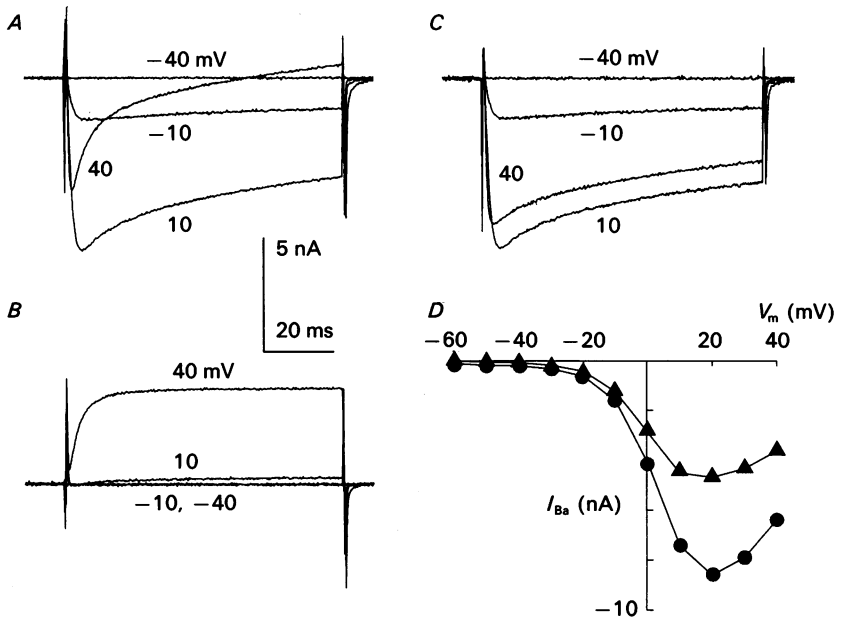

Fig. 1. Subtraction of background current and current–voltage relation for Ba^{2+} current. Membrane currents in one cell for four different step potentials before (*A*) and after (*B*) external application of 10 mM tetrapentylammonium (TPeA), and the difference records (*C*) showing the isolated Ba^{2+} current. At the end of each experiment, TPeA was used to block Ba^{2+} current and allow measurement of the outward proton current. Although the proton current is small at the standard test potential of 10 mV, this subtraction was performed in all subsequent experiments unless otherwise noted. *D*, current–voltage relation for Ba^{2+} current after subtraction of proton current. Peak current (●) and current at the end of the 80 ms depolarization (▲) are plotted against the step potential.

was minimized further by activating Ba^{2+} current at +10 mV where proton current was relatively small. Figure 1 shows the leak-subtracted currents before (*A*) and after application of TPeA (*B*), and the difference records (*C*) of isolated Ba^{2+} current. Unless otherwise noted, TPeA subtraction was applied to all data; Ba^{2+} and proton currents were measured using a step from a resting potential of −60 mV to +10 mV in Ba^{2+}–Tris saline. Figure 1*D* shows the current–voltage relation of the isolated Ba^{2+} current, obtained after subtracting both leak and proton currents.

Solutions

All concentrations given in this section are in millimolar units. Isolated neurons were placed in a 3 ml bath containing one of the following extracellular solutions at pH 7·4. *Lymnaea* saline: 50 NaCl, 2·5 KCl, 4 $CaCl_2$, 4 $MgCl_2$, 10 Hepes. Ba^{2+}–Tris saline: 4 $BaCl_2$, 4 $MgCl_2$, 76 TrisCl. Ca^{2+}–Tris saline: 4 $CaCl_2$, 4 $MgCl_2$, 76 TrisCl. Low-Ca^{2+}–Tris saline: 4 $MgCl_2$, 92 TrisCl. Low-Mg^{2+}–Tris saline: 4 $CaCl_2$, 92 TrisCl. The patch-clamp electrodes were filled with solutions containing Cs^+ (60), aspartate (28), and Hepes (60, pH 7·3). The electrode solution was identified according to additions to this basic solution as follows. DM–Ca^{2+} solution: 2 DM-nitrophen (tetra-sodium salt, Calbiochem), 2 ATP (di-sodium salt), 0·1 $MgCl_2$, 1·75 $CaCl_2$. DM–EGTA solution:

2 DM-nitrophen, 2 ATP, 1 $MgCl_2$, 1 EGTA. EGTA solution: 2 EGTA, 2 ATP, 0·1 $MgCl_2$, 1·75 $CaCl_2$. Where indicated, fluo-3 (10 or 100 μM, Molecular Probes, OR, USA) or dibromo-BAPTA (1 mM, Calbiochem) was added to these electrode solutions. Ca^{2+} calibration solutions were modified from Tsien & Rink (1980), and were labelled by their calculated Ca^{2+} concentrations. Each contained 12 NaCl, 60 CsOH, 28 aspartate, 100 Hepes. The Ca^{2+} ligands, added calcium, and pH were: 2 EGTA, 10 $CaCl_2$, and pH 7·3 for 8 mM Ca^{2+} solution; 10 NTA (nitrilotriacetic acid), 5 $CaCl_2$ and pH 7·4 for 0·1 mM Ca^{2+} solution; 10 HEDTA (*N*-hydroxyethylethylenediamine triacetic acid), 5 $CaCl_2$ and pH 7·7 for 1 μM Ca^{2+} solution; 10 EGTA, 5 $CaCl_2$ and pH 7·3 for 100 nM Ca^{2+} solution; 10 EGTA, 5 $CaCl_2$ and pH 7·8 for 10 nM Ca^{2+} solution; 2 EGTA, 0·1 Ca^{2+} (measured in stock caesium aspartate–Hepes solution) and pH 7·3 for 5 nM Ca^{2+} solution. The 8 mM Mn^{2+} solution contained 2 EGTA and 10 $MnCl_2$ at pH 7·3.

Photolysis of DM-nitrophen

The source of UV light used for photolysis of DM-nitrophen was a flash lamp built in the laboratory of Henry Lester at Caltech and lent to us for these experiments. This flash lamp was used in the experiments of Gurney, Tsien & Lester (1987) and is similar to that described by Rapp & Güth (1988). The discharge of a bank of capacitors (2100 μF) through a xenon arc bulb generated a flash with a falling time constant (τ) of 462 μs (Fig. 2*A*). This flash was filtered through the combination of a UV longpass filter (SCHOTT WG 295, PA, USA) and a UV bandpass filter (SCHOTT UG 11), and focused with quartz lenses (Oriel, CT, USA). The voltage of the discharge was set to the nearest volt as measured with a digital multi-meter (Beckman). The intensities of flashes obtained by charging to voltages from 50 to 400 V (Fig. 2*A*) were measured using the PMT arrangement described below (optical filters and lenses used with fluo-3 were removed), and were normalized to the intensity of the 400 V discharge (intensity of 400 V discharge = 100).

UV light was delivered to cells and test solutions in one of two arrangements. Both arrangements included the flash lamp housing (which contained the xenon bulb, reflective mirror, and quartz collecting lenses), the final quartz focusing lens (placed 32 mm above the cell), and a microscope. In the first arrangement, used exclusively to determine Ba^{2+} current block, the collecting lenses in the flash lamp housing were located 36 cm from the final focusing lens. This distance allowed us to move the microscope (dissecting type; Wild, Germany) into the light path to observe the cell. A foil mirror was placed underneath the patch-clamped cell, the microscope removed, and the final lens put into place before experiments. In the second arrangement, used to monitor both the concentration of Ca^{2+} and the block of Ba^{2+} current, the collecting lenses were located only 12 cm from the focusing lens. An inverted microscope (described below) provided the optics needed during patch clamp manipulations and for monitoring Ca^{2+}, as well as aid in focusing and centring the UV light for photolysis. The intensity of UV light reaching cells in this second arrangement may not be the same as that reaching cells in the first. In the second arrangement, foil cannot be placed underneath the cell, possibly reducing cell UV exposure by as much as 50%, but in this arrangement the final focusing lens collects a somewhat larger fraction of the light coming from the collecting lenses. Judging from the amount of Ba^{2+} current blocked, these two changes roughly cancel.

Using the stability constants of Martell & Smith (1974) and the dissociation constants (K_d) for DM-nitrophen given by Kaplan & Ellis-Davies (1988) we wrote programs to simultaneously solve the multi-buffer/ligand equations and calculate the expected free Ca^{2+}. These programs predict that the Ca^{2+} of an unphotolysed DM–Ca^{2+} solution (see above for composition) should be 51 nM and will increase to 0·3 mM after complete photolysis. To model the magnitude and time course of both Ca^{2+} release from DM-nitrophen and channel block by intracellular Ca^{2+}, we wrote programs which used first-order binding kinetics to calculate concentrations of all buffers and metals. Forward rate constants (K_f) were estimated from similar compounds when available and adjusted to fit experimental results.

Monitoring intracellular Ca^{2+}

Calcium-sensitive electrodes and the optical indicator fluo-3 were used to measure Ca^{2+}; both were calibrated using the calibration solutions described above. Calcium electrodes were similar in construction to those used by Byerly & Moody (1984). Briefly, VWR micropipette glass was pulled to a tip diameter of < 1 μm (Narishige PE-2 puller), silanized, and then back-filled with 70%

ethanol. Ethanol was replaced with the 10 nM calibration solution. The tip was dipped into Ca^{2+}-ionophore cocktail 1A (Fluka) while applying negative pressure to the opposite end of the electrode, filling the tip with 40–60 μm of ionophore cocktail. Electrodes were soaked in the 10 nM calibration solution for 1 h before use and used only that day. Some electrodes had response time constants as fast as 100 ms, determined by their response after photo-release of Ca^{2+}.

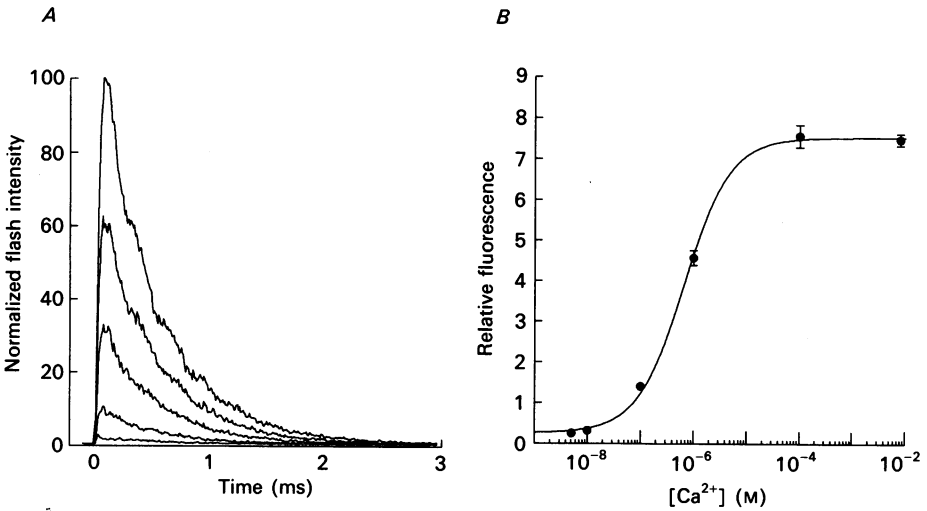

Fig. 2. Measurement of UV flash intensity and time course and calibration of fluo-3. *A*, capacitors with a total capacitance of 2100 μF were charged to 400, 300, 200, 100 and 50 V then discharged through a xenon arc lamp. Flashes were filtered to pass a band of UV light centred around 350 nm (65 nm half-width), then measured with a photo-multiplier tube. The peak intensity of the largest (400 V) flash was arbitrarily designated 100. *B*, fluorescence of 10 μM fluo-3 was measured in calibration solutions containing 5 nM to 8 mM free Ca^{2+}, and one containing 8 mM Mn^{2+} (see *Solutions*). The fluorescence ratio of each calibration solution to that of the Mn^{2+} solution is plotted against the $[Ca^{2+}]$ in each solution (error bars indicate standard error when larger than the symbol, $n = 7$–15). Fluorescence was measured using a confocal arrangement with a 1×5 μm volume. The smooth line is a fit (expression given in the text) to this data, which was then used to calibrate subsequent measurements of fluo-3 fluorescence.

Fluo-3 fluorescence was measured in a confocal arrangement using pinholes of 50 μm or 1 mm in diameter (Melles-Griot, CA, USA), a photomultiplier tube (PMT, Hamamatsu R955, NJ, USA) and power supply (Ealing Electro-optics, MA, USA), and an inverted microscope (Nikon Diaphot, xenon epi-fluorescence attachment, 40× oil immersion objective). The source pinhole, through which excitation light passed, was placed in the field diaphragm of the Nikon epi-fluorescence unit. The detector pinhole was positioned in front of the PMT (mounted on the Nikon camera port) at the image plane. Pinholes were aligned to give a maximal signal at the PMT when monitoring Ca^{2+}-saturated fluo-3 fluorescence between coverslips (< 1 μm thick). Excitation light was limited to a 470–490 nm band (Nikon filter block B-1A) to prevent photolysis of DM-nitrophen. The 1 mm pinholes allowed measurement of fluorescence from a 25×25 μm volume (diameter × depth) and were used for most intracellular measurements. The 50 μm pinholes allowed measurement from a $1{\cdot}25 \times 5$ μm volume and were used primarily for extracellular measurements. The depth of the volume from which fluorescence was collected was determined from the change of fluorescence measured on focusing past the interface of glass and a fluorescent drop. Figure 2*B* shows the calibration curve obtained for our intracellular solutions containing 10 μM fluo-3. The relative fluorescence (fluorescence of each calibration solution divided by the fluorescence of the Mn^{2+} solution) is plotted against the free Ca^{2+} of each calibrating solution. The volume of the calibration

solution from which fluorescence was measured was held constant by use of the 50 μm pinholes. This data was fitted (continuous line) to the equation $[Ca^{2+}] = K_d(R-R_{min})/(R_{max}-R)$, where R is the relative fluorescence. The fitted constants are: K_d, 656 nM; R_{min}, 0·27; and R_{max}, 7·53.

Intracellular Ca^{2+} was determined in cells dialysed with DM–Ca^{2+} solution containing the same concentration of fluo-3 (10 μM). The background fluorescence of the neuron was measured before the patch membrane was broken. The interior of the cell was allowed to equilibrate with the electrode solution for more than 15 min before measuring the baseline and flash-induced fluorescence transients. The reference level of fluorescence, equivalent to 74 nM Ca^{2+}, was determined by saturating fluo-3 with Mn^{2+} (Kao, Harootunian & Tsien, 1989). At the end of an experiment, enough Mn^{2+} was added to the bath for a final concentration of 4 mM, and then fluorescence was monitored for 10–20 min until stable. The most stable Mn^{2+} loading was obtained without additional membrane permeabilization, although equivalent results were obtained using ionomycin or brief, extreme hyperpolarization (100–200 mV for 50 ms). The presence of saturating Mn^{2+} in the cell was verified by flashing the cell and observing that the flash transient was identical to that obtained in an unloaded cell. These flash transients were independent of fluo-3 fluorescence and were subtracted from records taken when monitoring fluo-3 fluorescence.

In one set of experiments designed to detect a fast Ca^{2+} spike with a duration of only tens of milliseconds, the concentration of fluo-3 was increased to 100 μM and three blue–green bandpass filters (SCHOTT BG 39) were placed before the PMT. These filters reduced the intensity of light from flashes that leaked to the PMT, thus shortening the duration of PMT saturation. Fluorescence of extracellular droplets was monitored without the standard confocal arrangement, using a coverslip to limit the volume of the solution. Intracellular measurements were made using the standard 25 × 25 μm confocal arrangement. UV flashes were shortened (falling τ of 134 μs) in both cases by charging only 263 μF with 750 V.

RESULTS

Block of Ba^{2+} current by photo-released Ca^{2+}

Barium was chosen over calcium as the charge carrier in these experiments to minimize current-dependent inactivation of the Ca^{2+} channel current and loading of DM-nitrophen near the membrane by divalents entering through Ca^{2+} channels. Ba^{2+} current exhibits less inactivation than Ca^{2+} current and the affinity of DM-nitrophen for Ba^{2+} is less than that for Ca^{2+} ($\approx$ 700 times less in the parent compound EDTA). In these *Lymnaea* neurons at +10 mV Ba^{2+} currents decayed 36% ($n = 24$) over the 70 ms period following the peak current, while Ca^{2+} currents decayed 69% ($n = 9$). Current-dependent inactivation of Ca^{2+} channels is thought to be due to accumulation of Ca^{2+} entering through Ca^{2+} channels (Eckert & Chad, 1984); since this accumulation is too localized to measure, we avoid this complication by using Ba^{2+} as the charge carrier.

Neurons patch clamped in the whole-cell configuration with an electrode containing DM–Ca^{2+} solution were flashed with maximal intensity UV light. Two types of experiments were performed to determine the block of Ba^{2+} current by intracellular Ca^{2+}. In one type, the flash was triggered after Ba^{2+} current was activated (Fig. 3*A*), directly revealing the early time course of block. In the second type, the flash was triggered before activating Ba^{2+} current (Fig. 3*B*) and then peak Ba^{2+} current was measured; this minimized both the problem of separating block from inactivation and the possibility of DM-nitrophen loading with Ba^{2+}. When Ba^{2+} current was activated before triggering the flash, a rapidly developing reduction of current was observed; Fig. 3*A* shows the average of eight such experiments. When measured at the end of the 80 ms depolarization, Ba^{2+} current was blocked 49 $\pm$ 15% (mean $\pm$ standard deviation, $n = 8$) compared to the control current (recorded 10 s

earlier). A correction for the slight reduction of Ba^{2+} current between depolarizations (less than 1 % for depolarizations separated by 10 s) due to inactivation and wash-out was applied to this and all subsequent data. Figure 3*B* shows the average current for eight experiments of the second type, in which the flash was triggered 50 ms before

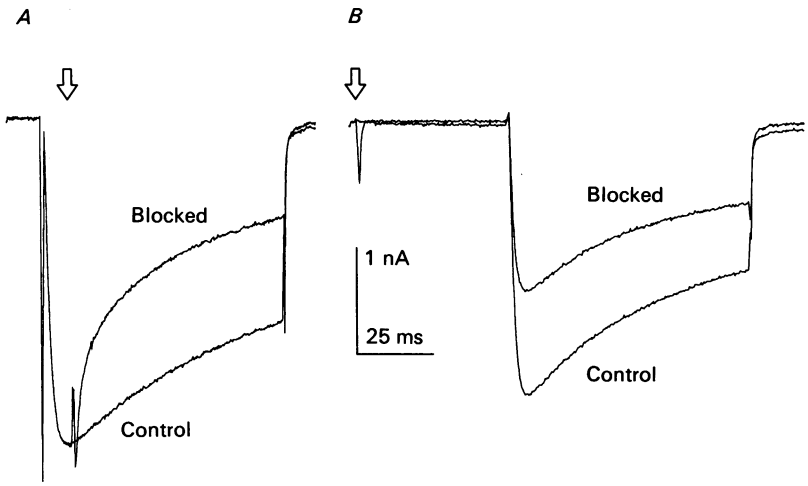

Fig. 3. Ba^{2+} current blocked by photolysis of Ca^{2+}-loaded DM-nitrophen. Isolated neurons were patch clamped in the whole-cell configuration with an electrode containing Ca^{2+}-loaded DM-nitrophen, then exposed to a maximal flash of UV light. Flashes were triggered (onset at arrows) either during an 80 ms depolarization to +10 mV (at a holding potential of −60 mV) (*A*), or 50 ms before the depolarization (*B*). These potentials are used for measuring Ba^{2+} current in all of the following figures unless stated otherwise. Control current was measured 10 s before each flash. Currents shown are the average of eight cells.

activating Ba^{2+} current. Control current was again measured 10 s before the flash. The block of the peak Ba^{2+} current measured for these experiments was 42 ± 13 %. The difference in the magnitude of block measured in the two types of experiments was not due to a difference in time from the flash, since in both experiments block was measured at roughly the same time after the flash. Block measured at the end of the 80 ms depolarization in this second type of experiment was higher (47 ± 8 %) and nearly the same as that measured at the end of the depolarization in the first type of experiment.

The apparent block of Ba^{2+} current described above could also result from a Ca^{2+}-activated outward current. To test this possibility, neurons in which the Ba^{2+} current had washed out were stepped to the same potential and flashed. In seven of seven cells, no current was activated by the flash that could make a significant contribution to the apparent block of Ba^{2+} current. A small, slowly activating leak current does seem to appear with flashes on DM–Ca^{2+}-loaded cells, as can be seen before the voltage step in Fig. 3*B* and after the voltage step in both Fig. 3*A* and *B*. This current disappears some time before the next voltage step, 10 s later.

The Ba^{2+} current surviving the block by intracellular Ca^{2+} had the same voltage dependence and inactivation kinetics as did the Ba^{2+} current before block. A voltage

ramp from −50 to +50 mV was applied over 182 ms. Ten seconds after the first ramp a flash of maximal intensity was triggered, and then 15 ms later a second ramp was applied. Figure 4*A* shows the results of one such experiment, plotted as a current–voltage relation. No shift in channel voltage dependence is seen in this

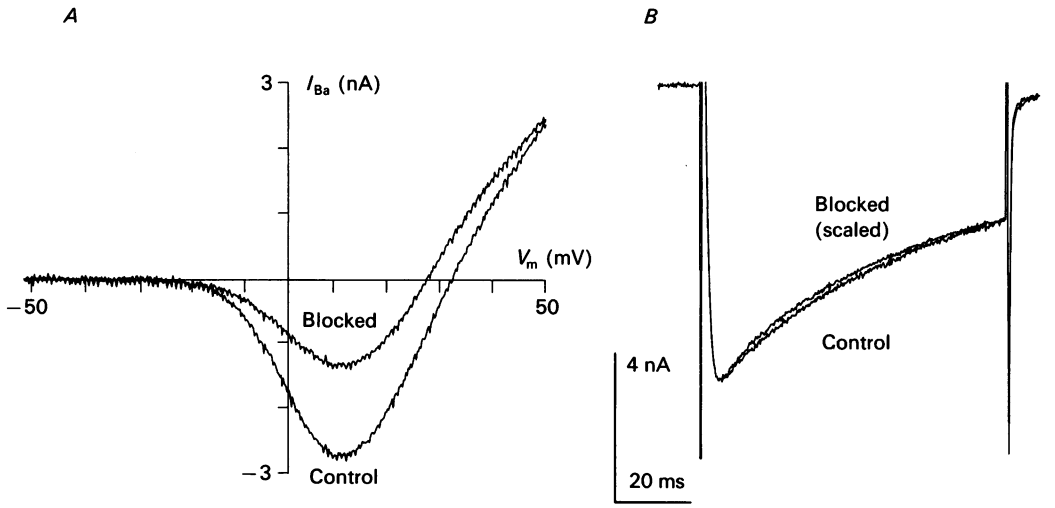

Fig. 4. Effect of block on Ba^{2+} current voltage dependence and inactivation. *A*, a voltage ramp of approximately 0·5 mV ms^{-1} was applied before and after a flash. The two ramps were separated by 10 s with the flash occurring 15 ms before the start of the second ramp. Seven cells gave similar results. The outward proton currents have not been subtracted from these records (see Methods). *B*, time course of control and blocked currents. Currents are averages from six cells in which the blocked current 1 s after a flash is scaled to the control level. Proton currents have been subtracted from these records. Current scale applies to control current. The rate of inactivation did not significantly change with block ($n = 9$).

experiment or six repetitions. Proton currents have not been subtracted from these records. Inactivation was studied for Ba^{2+} currents recorded before and 1 s after the flash, at which time 36% of the Ba^{2+} current is blocked. The time constant of inactivation, determined from a single exponential fit to the decaying phase of the current, did not reveal a significant difference between the two groups (control, 40 ± 11 ms; blocked, 39 ± 10 ms; $n = 9$). In Fig. 4*B*, averages of the Ba^{2+} currents from six cells are shown. The peak of the blocked current has been scaled to the control level, to allow a better comparison of inactivation.

As is apparent from Fig. 3*A*, the block of Ba^{2+} current occurs within milliseconds of the Ca^{2+}-releasing flash. To measure the precise time course of the block, we performed a series of experiments like that shown in Fig. 3*B*, in which the time between flash and voltage step was varied between 1 ms and 1 s. Control currents were measured 10 s before each flash. The results of these experiments are shown in Fig. 5*A*. Percentage block ($n = 5$–8) is plotted against the time between the flash and the measurement of current. Since only a few episodes of block could be measured in

each cell (see below), and variations in the magnitude of block between cells might obscure the time course of Ba^{2+} current block, the block measured 1 s after a flash was determined in each cell and used to normalize block measured at different time points. Measurements from each cell were normalized such that the block at 1 s for

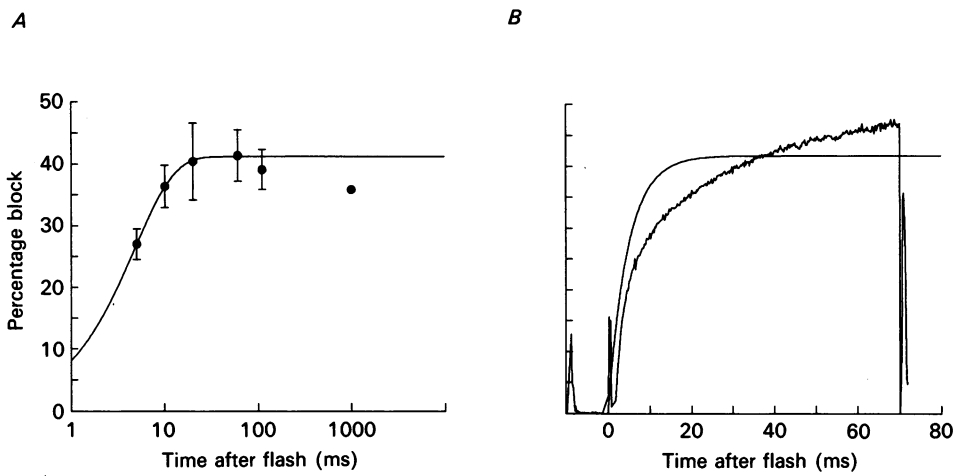

Fig. 5. Time course of current block. *A*, time course determined for peak Ba^{2+} current. The interval between flash and depolarization was varied between 1 ms and 1 s, while control current was measured 10 s before the flash. When more than one flash was applied to a cell, flashes were separated by at least 7 min. Currents were measured at the times indicated, within 2 ms of the peak current. Measurements from each cell were normalized to the block at 1 s before averaging (n = 5–8). Error bars indicate standard error. The continuous line represents a single exponential fit to the 5–60 ms averages (τ = 4·7 ms). *B*, time course of block determined from flashes occurring during Ba^{2+} current. Data from Fig. 3*A* is converted to percentage block and plotted *versus* time from flash. The smooth line shows the fit in Fig. 5*A* on this linear time scale.

a cell was equal to the mean value of 36%. The two earliest time points were taken from the same set of experiments in which Ba^{2+} current was activated 1 ms after flashes; both current measurements were made within 2 ms of the peak current. Successive flashes were separated by at least 7 min to allow the cell to return to its steady state, and the order of time intervals was randomized. A single exponential fit to the first four points (5–60 ms) has a τ of 4·7 ms and is shown as a continuous line in Fig. 5*A*.

Figure 5*B* (noisy trace) shows the average time course of block measured during an 80 ms depolarization to +10 mV, a depolarization which considerably inactivates the control Ba^{2+} current. The data come from the experiments shown in Fig. 3*A*. For comparison, the exponential fitted to the data of Fig. 5*A* is also plotted in Fig. 5*B* (smooth line). There is fairly good agreement between the two measures of percentage block though early times appear to be underestimated and later times overestimated in this second measure. Control experiments described in the next section revealed a light-induced current transient (Figs 7 and 8) which partially explains the differences. This current transient has a fast inward component and a

slowly developing outward component similar in magnitude to the differences between block measured at the peak and end of current pulses. In all likelihood, the experiments summarized in Fig. 5*A* most accurately reveal the time course of the block, since they are not contaminated by this flash-induced current transient, and

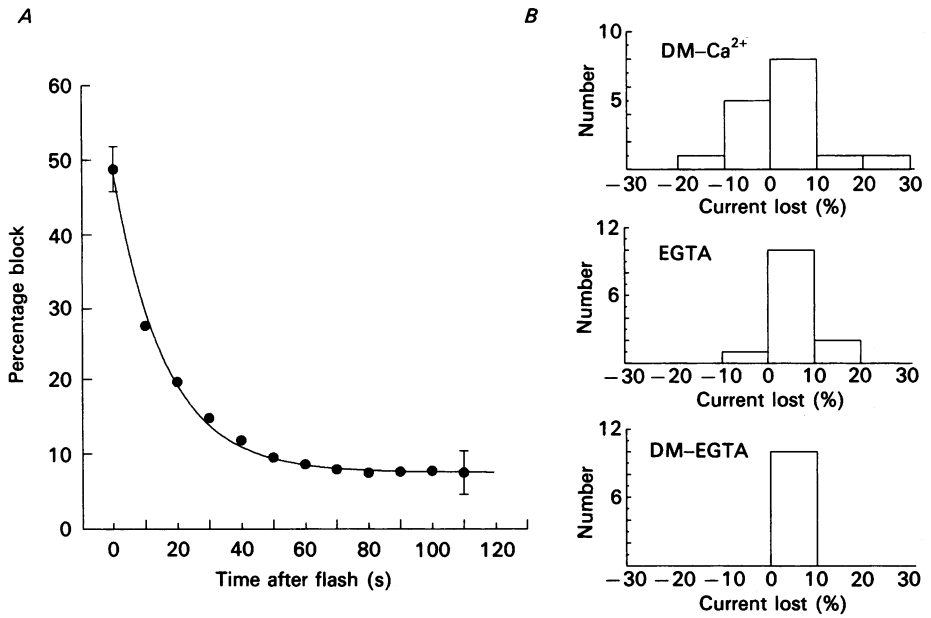

Fig. 6. Recovery from block. *A*, average percentage block (±standard error) of sixteen cells monitored every 10 s after a maximal flash. Block was measured at the end of each 80 ms depolarization. A single exponential fit to the averages had a τ of 16 s (continuous line). *B*, histogram of maximum recovery from the same sixteen cells (DM–Ca^{2+}) and from cells under two control conditions (EGTA, DM–EGTA). Negative values indicate enhancement of current, while positive ones indicate incomplete recovery.

are based on measurements of peak Ba^{2+} current, which has a constant level of voltage-dependent inactivation.

Recovery from block was three orders of magnitude slower than development of block. Recovery was determined by measuring the Ba^{2+} current at the end of 80 ms depolarizations applied every 10 s after a flash. In Fig. 6*A*, the percentage block, calculated from these currents and the control current recorded 10 s before the flash, is plotted against time following the flash ($n = 16$). Single exponential fits to each measured recovery had an average time constant of 16±6 s (continuous line in Fig. 6*A*). After a maximal intensity flash, Ba^{2+} currents recovered to within 4·1±9·5% of their original size. Figure 6*B* (top) is a histogram of the maximum recovery, expressed as percentage current lost, for these same sixteen cells. In six of the sixteen cells studied the Ba^{2+} current recovered completely or transiently rose above pre-flash levels, while in other cells the recovery of the Ba^{2+} current was poor. Multiple flashes of the same intensity applied to one cell showed no trend towards increasing or decreasing block. However, cells could not withstand more than four exposures to

the highest intensity flash. Excess flashes caused them to suddenly become too leaky for further recording. As discussed below, this result was apparently not due to the effects of UV flashes alone but to the photo-release of Ca^{2+}.

Ca^{2+}-independent effects of flash on Ba^{2+} current

The block of Ba^{2+} current seen on photolysis of Ca^{2+}-loaded DM-nitrophen could possibly be due to effects of UV light other than the release of Ca^{2+}. The UV flash

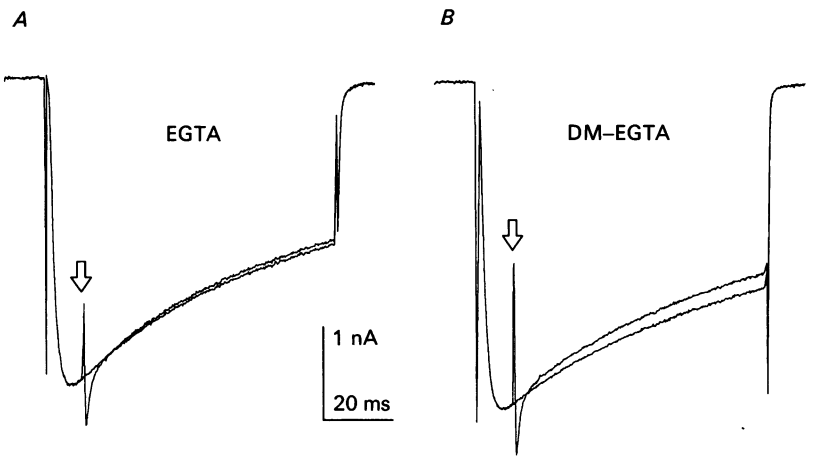

Fig. 7. Ca^{2+}-independent current transient induced by UV light. Ca^{2+}-loaded DM-nitrophen (DM–Ca^{2+}) in the intracellular solution was replaced by either EGTA or a mixture of unloaded DM-nitrophen and EGTA (DM–EGTA). Maximal flashes were triggered at the time indicated by arrows. *A*, average control and blocked currents from ten EGTA-containing cells. *B*, average currents from seven DM–EGTA cells.

might have direct effects on the Ba^{2+} current, independent of DM-nitrophen photolysis, and photo-products other than Ca^{2+} (fragments of the DM-nitrophen molecule and Mg^{2+}) might block the Ba^{2+} current. The direct, damaging effect of the unfiltered flashes on the cells was minimized by blocking wavelengths above and below those most effective in photolysing DM-nitrophen (near 350 nm). More than 99% of the radiation below 275 nm and of that above 400 nm was removed by filtering (see Methods). Without this optical filtering cells became too leaky to record from during a single, maximal intensity flash.

To determine the effects of the flash without DM-nitrophen, Ca^{2+}-loaded DM-nitrophen in the intracellular solution was replaced by a photo-insensitive buffer (EGTA). Using this intracellular solution and the standard optical filtering, a cell could withstand more than twenty maximal intensity flashes. In Fig. 7*A* a flash-induced fast current transient followed by a slight reduction in Ba^{2+} current can be seen in cells dialysed with EGTA solution (average of ten cells). The reduction in Ba^{2+} current measured at the end of the depolarization was $3{\cdot}0 \pm 1{\cdot}8\%$. Experiments on EGTA-loaded cells using the same protocol shown in Fig. 3*B*, where flashes were triggered 50 ms before the depolarization, revealed a 1·1% reduction of peak current and a 6·2% reduction of current at the end of the 80 ms depolarization ($n = 4$). In

these experiments the slowly developing inward leak current seen in cells loaded with DM–Ca^{2+} solution (Fig. 3) was not observed.

To determine the effects of photo-products other than Ca^{2+}, a combination of EGTA and Ca^{2+}-free DM-nitrophen was used (DM–EGTA solution). Since the nominally Ca^{2+}-free stock solution contained less than 0·1 mM free Ca^{2+}, 1 mM EGTA was added to minimize DM-nitrophen Ca^{2+}-loading. DM-nitrophen was less than 5% Ca^{2+}-loaded in DM–EGTA solution compared to 93% in standard DM–Ca^{2+} solution. Figure 7*B* shows the results of flashes applied to cells dialysed with DM–EGTA solution. The reduction of current in this averaged record was 7·1 ± 2·4% at the end of the current pulse ($n = 7$). Ba^{2+} current was reduced by 3·5% at the peak and 6·5% at the end of the current pulses ($n = 3$) in cells which were flashed 50 ms before the depolarization. The increased reduction of Ba^{2+} current with DM–EGTA solution (Fig. 7*B*) compared to that with EGTA solution (Fig. 7*A*), especially during the first 70 ms following the flash, may be due to a small Ca^{2+} photo-release or to other photo-products. Mg^{2+}, which is calculated to jump from 3 to 6 μM following the flash, has been reported to weakly block Ca^{2+} current in these cells when millimolar levels are applied by change of the electrode (internal) solution (Byerly & Yazejian, 1986). In any case, none of these relatively small effects of UV flashes or photo-products could explain the significant Ba^{2+} current block which occurred with DM–Ca^{2+} solution.

Following flashes that released little, if any, intracellular Ca^{2+} (EGTA or DM–EGTA solutions) the average irreversible loss of Ba^{2+} current was about the same as for experiments in which Ca^{2+} was released (DM–Ca^{2+} internal solution). Figure 6*B* shows the distributions of Ba^{2+} current loss, calculated from the magnitudes of the Ba^{2+} currents just before the flash and about 1 min after the flash when maximal recovery had occurred. Ba^{2+} current in DM–Ca^{2+} cells recovered from approximately 50% block to values ranging from 25% current loss to 12% enhancement. DM–EGTA cells recovered from 7% block to values of 6–1% current lost. The average current lost was similar for each internal solution: DM–Ca^{2+}, 4·1 ± 9·5% ($n = 16$); EGTA, 4·9 ± 4·9% ($n = 13$); DM–EGTA, 3·8 ± 1·8% ($n = 10$).

Two components of the Ca^{2+}-independent effects of flashes (shown in Fig. 7) are current dependent. Flashes cause a fast outward electrical transient, then a brief inward current followed by a slower outward current component. By flashing cells after stepping to different potentials, we were able to determine the voltage and current dependence of the flash-induced transients. Figure 8 shows the results of two such experiments, one on a cell with Ba^{2+} current (Fig. 8*A* and *B*) and the other on a cell without Ba^{2+} current (Fig. 8*C* and *D*). Figure 8*B* and *D* shows the flash-induced transients obtained by subtracting the currents recorded without flashes from those recorded during flashes. A prominent brief inward current followed by a prolonged outward current is seen at +20 mV in the cell with Ba^{2+} current (Fig. 8*B*), but not in the cell lacking Ba^{2+} current (Fig. 8*D*). At +60 mV, where the current is primarily carried by protons, flashes induce a brief outward current transient followed by a prolonged outward current. There was no measurable reduction in proton current amplitude 10 s after flashes. When flashes were applied 1 ms before depolarizations activating proton or Ba^{2+} current, only the brief inward current transient occurred. Thus, these Ca^{2+}-independent flash-induced transients depend more on the current flowing at the time of the flash than on the membrane potential.

The origin of these Ca^{2+}-independent flash-induced transients is not clear. Flashes on the tips of electrodes alone (no cell) induce transients in the current records, which often have a time course similar to those seen in Fig. 8. The transients induced in cell-free electrodes are also strongly current dependent. The size of the transient is

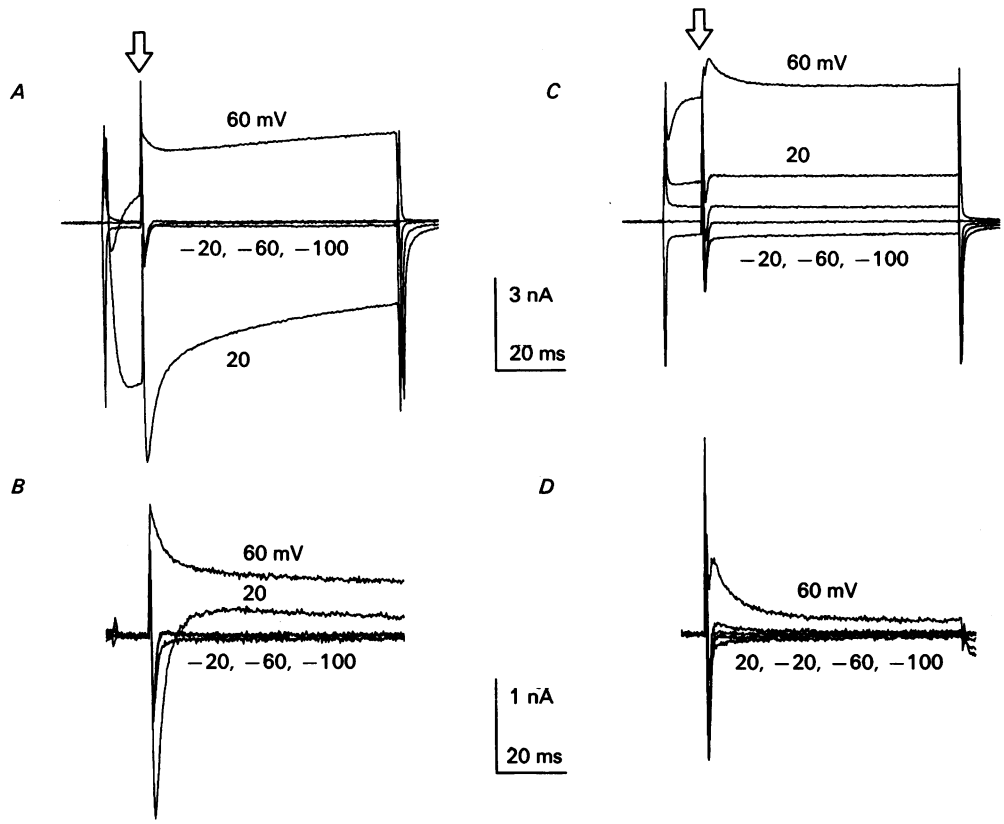

Fig. 8. Current dependence of Ca^{2+}-independent current transient. Flashes were triggered (onset at arrows) after depolarizing the membrane to the indicated potentials. Each depolarization was separated by 1 min. Neither proton nor leak currents were subtracted. Currents from an EGTA-containing cell before (*A*) and after (*B*) subtracting control (unflashed) currents ($n = 5$). Note prominent current transient at +20 and +60 mV. Currents from an EGTA-containing cell which did not show any Ba^{2+} current, before (*C*) and after (*D*) subtracting control currents ($n = 8$). Note the absence of the current transient at +20 mV.

proportional to the size of the current flowing at the time of the flash, and the direction of the transient is the same as that of the current flowing before the flash. The reversal of the current transient direction with current direction is not consistent with the hypothesis that flashes induce a change in voltage. Measurement of the potential in voltage-clamped cells with a microelectrode revealed only a slight depolarization (less than 1 mV) during flashes, which could not account for the transient. Due to the complicated time course and current dependence of this transient, we have not attempted to subtract it from the currents recorded during

flashes that did release Ca^{2+}. As a result, we have more confidence in the time course of the block shown in Fig. 5*A*, where the flash occurs before Ba^{2+} current is activated, than that in Fig. 5*B*, which is contaminated by the flash-induced current transient.

Measurement of photo-released Ca^{2+}

Direct measurement of intracellular Ca^{2+} was essential in this study. Previous studies have shown that when supplied with ATP, these neurons can maintain intracellular Ca^{2+} at levels considerably lower than that in strongly buffered dialysis solutions (Byerly & Moody, 1984). In addition, the strength of the endogenous Ca^{2+} buffering has not been quantitatively measured in these neurons. Therefore, it is not reasonable to assume that the Ca^{2+} loading of DM-nitrophen in the cell is the same as it is in the dialysing solution, nor is it possible to predict what fraction of the Ca^{2+} released by photolysis will remain free. We used two methods to measure Ca^{2+} in this study. Calcium-sensitive electrodes were used primarily to measure free Ca^{2+} in extracellular droplets of the DM–Ca^{2+} solution and to verify measurements made with the optical indicator fluo-3. Fluo-3 was used to measure Ca^{2+} in both droplets and cells. It was chosen over other optical Ca^{2+} indicators due to its relatively low affinity for Ca^{2+}, ability to measure higher concentrations of Ca^{2+} than fura-2, a high signal-to-noise ratio (40-fold increase in fluorescence after calcium binding), and a longer excitation wavelength which minimizes photolysis of DM-nitrophen.

UV flashes on droplets of DM–Ca^{2+} solution produced large increases in Ca^{2+}. When measured with Ca^{2+}-sensitive electrodes, maximal intensity flashes on droplets increased Ca^{2+} to 59 μM from an initial concentration of 42 nM ($n = 6$). Measurements using fluo-3 and the fine-resolution confocal arrangement (50 μm pinholes, see Methods) indicated a step increase in Ca^{2+} from 113 ± 12 nM ($n = 52$) to 41 ± 7 μM ($n = 11$) under the same conditions. Figure 9*A* (■) shows the relation between the Ca^{2+} concentration, determined using fluo-3, and the relative intensity of the UV flash. The free Ca^{2+} concentration in the unflashed DM–Ca^{2+} solution is consistent with the binding constants of all the calcium buffers and the composition of DM–Ca^{2+} solution, if it is assumed that 5·6% of the added DM-nitrophen was photolysed before flashes. Such an error in the unphotolysed DM-nitrophen concentration is more plausible than other explanations since there was some evidence for breakdown of DM-nitrophen under our use and storage conditions. The continuous line drawn in Fig. 9*A* shows the expected Ca^{2+} concentration following photolysis, assuming that the rate constant for photolysis is proportional to the flash intensity and that the maximal flash brought the total photolysis of DM-nitrophen to 31%. The maximal flash produces Ca^{2+} levels that almost completely saturate the fluo-3 fluorescence.

When *Lymnaea* neurons were dialysed with DM–Ca^{2+} solution, intracellular Ca^{2+} was strikingly different from that measured in droplets of the same solution. The steady-state concentration of Ca^{2+} measured in neurons was 36 ± 43 nM ($n = 13$), compared to 113 nM measured in droplets. In contrast to the step increase produced in extracellular droplets, flash photolysis of DM-nitrophen in neurons produced an intracellular Ca^{2+} transient, which decayed with three time constants of 120 ms, 2 and 13 s. Figure 9*B* shows the first 5 s of this Ca^{2+} transient following a maximal flash. The return of intracellular Ca^{2+} to the steady-state value is presumably due to Ca^{2+} sequestration and pumping by the cell and to on-going dialysis with the

electrode containing unphotolysed DM–Ca^{2+} solution. Intracellular Ca^{2+} measured as early as possible after the maximal flash (20 ms) was 126 ± 23 nM ($n = 10$) compared to 41 μM in droplets (Fig. 9*A*). One reason for the attenuated rise in intracellular Ca^{2+} after photolysis is the unloading of Ca^{2+} from DM-nitrophen that occurs prior to

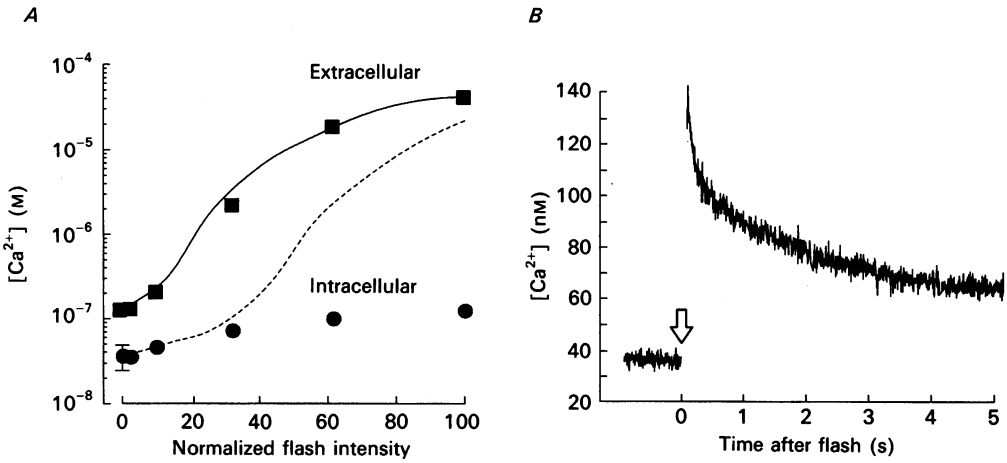

Fig. 9. Free Ca^{2+} following flash photolysis of DM-nitrophen. *A*, comparison of extracellular and intracellular Ca^{2+} photo-release. ■, free Ca^{2+} in extracellular droplets of DM–Ca^{2+} solution after flashes of each intensity (Fig. 2*A*). Fluorescence was measured with a confocal arrangement (1×5 μm volume) and calibrated by saturating fluo-3 (10 μM) with Ca^{2+}. Since maximal intensity flashes nearly saturated fluo-3, Ca^{2+} for this point was calculated using the flash intensity–photolysis relation determined for smaller flashes ($n = 10$–11 for each flash intensity and 52 for the level before flashes). The continuous line represents the predicted relation between free Ca^{2+} and flash intensity assuming the photolysis rate constant is proportional to flash intensity (see text). ●, intracellular Ca^{2+} measured as early as possible after flashes of each intensity (averages of 9–10 cells each). Ca^{2+} before each flash was normalized to the baseline average of 36 nM ($n = 13$). Error bars on this first point indicate standard error. The dashed line represents the predicted relation given the initial intracellular [Ca^{2+}] and the flash intensity–photolysis relation determined from extracellular DM–Ca^{2+} solution (■——■). *B*, time course of intracellular Ca^{2+} after maximal intensity flashes. Each point in this record represents an average from three cells over a 5 ms period. The gap in the record due to the flash (onset at arrow) is 20 ms in duration.

flashes (described above). In Fig. 9*A*, the dashed line indicates the expected Ca^{2+} levels following photolysis, allowing for the reduced Ca^{2+} loading of DM-nitrophen in the cell. The filled circles in Fig. 9*A* indicate measured peak intracellular Ca^{2+} following flashes of each intensity. The rise in intracellular Ca^{2+} produced by photolysis is only about one-hundredth of the expected amount. Three experiments in which Ca^{2+}-sensitive electrodes were used also indicated submicromolar elevation of intracellular Ca^{2+} following maximal flashes.

The most reasonable explanation for the small increase in intracellular Ca^{2+} following photolysis of DM-nitrophen is that endogenous buffers bind almost all the photolytically released Ca^{2+}. The other possible explanations seem to have been ruled out. An attenuated rise in intracellular Ca^{2+} might result from strong absorption of

UV light by the cell or extracellular bath. However, the Ca^{2+} rise in droplets placed under the same depth of extracellular solution was not attenuated, and localized measurements of intracellular Ca^{2+} using the fine-resolution confocal arrangement (see Methods) did not indicate a significant gradient of Ca^{2+} release across the cell. Intracellular Ca^{2+} after maximal intensity flashes was compared in the same 50 μm cell at both the back surface, where UV light must penetrate the entire diameter of the cell, and front surface (top or side of cell), where light passes through only a few micrometres of membrane and cytosol. The peak elevation in Ca^{2+} varied by less than 30% between front and back, exhibiting no systematic bias towards more release at the front. The small elevations of intracellular Ca^{2+} evoked by flashes might also result from interference from Mg^{2+} or Ba^{2+}, which are present in the extracellular solution and presumably accumulate to an unknown extent inside the dialysed cell. Intracellular Mg^{2+} might displace Ca^{2+} from DM-nitrophen, and Ba^{2+} quenches fluo-3 fluorescence. However, neither possibility seems to occur, since the measured jump of intracellular Ca^{2+} in response to photolysis is unchanged when the extracellular solution contains no Ba^{2+} (Ca^{2+}–Tris saline or low-Ca^{2+}–Tris saline) or no Mg^{2+} (low-Mg^{2+}–Tris saline). The presence of endogenous buffers in these neurons is not surprising; it is well known that neurons contain many proteins with a high affinity for Ca^{2+} (Sala & Hernandez-Cruz, 1990). As expected if endogenous buffers are taking up most of the photo-released Ca^{2+}, we found that increasing the concentration of DM-nitrophen to 10 mM increased the magnitude of the jumps in intracellular Ca^{2+} by 34% ($n = 8$).

We believe the intracellular Ca^{2+} concentrations we measure are representative of those that block the Ca^{2+} channels. The endogenous buffers in these neurons appear to rebind the photo-released Ca^{2+} exceedingly rapidly, apparently so rapidly that no large intracellular Ca^{2+} spike occurs immediately following the flash. We base this conclusion on two types of evidence. One is that we see no indication of an intracellular Ca^{2+} spike when monitoring fluo-3 fluorescence within 2 ms of the flash. Due to the intensity and duration of flashes used to photolyse DM-nitrophen, the Ca^{2+} concentrations presented in Fig. 9 were measured no earlier than 20 ms following flash onset; however, higher Ca^{2+} concentrations may exist immediately after flashes if free, unphotolysed DM-nitrophen is slow to bind Ca^{2+} (Grell, Lewitzki, Ruf, Bamberg, Ellis-Davies, Kaplan & DeWeer, 1989). Since rate constants for the binding of DM-nitrophen to Ca^{2+} are not available, we attempted to measure directly this possible Ca^{2+} spike in droplets of DM–Ca^{2+} solution. A brief flash, obtained by reducing the capacitance storing the flash current to one-eighth of normal, allowed the measurement of fluo-3 fluorescence within 2 ms following flash onset. As shown in Fig. 10*A*, the fluo-3 fluorescence exhibits a transient which decays with a 15 ms time constant. Using a computer model that includes the time course of the flash and kinetics of all the binding reactions to calculate the time course of the Ca^{2+} spike, the fluorescence transient of Fig. 10*A* allows us to estimate the forward rate constant for Ca^{2+} binding to DM-nitrophen to be about 5×10^7 M^{-1} s^{-1}. The surprisingly slow time course of this Ca^{2+} spike is due to the use of 100 μM fluo-3 in this experiment to increase the intensity of the fluorescence. The Ca^{2+} released by photolysis is first taken up by fluo-3, which binds rapidly (1×10^9 M^{-1} s^{-1}; Eberhard & Erne, 1989), and then slowly transferred to the higher affinity DM-nitrophen. Thus, in droplets, flash

photolysis of DM-nitrophen does not produce a simple step change in Ca^{2+}, but instead includes an initial, rapid, over-shooting spike. In contrast, Fig. 10*B* shows the average of the fluo-3 signals recorded from twenty-nine brief flashes on cells containing DM–Ca^{2+} solution. All conditions are the same in this experiment as in

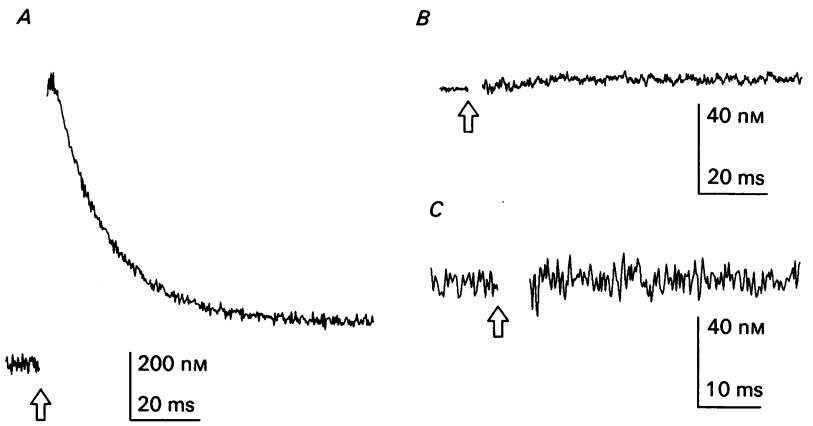

Fig. 10. Early time course of free Ca^{2+} following photolysis. *A*, Ca^{2+} spike after partial photolysis of DM-nitrophen in droplets (extracellular). DM–Ca^{2+} solution containing 100 μM fluo-3 was exposed to a brief flash (falling $\tau = 134$ μs) while monitoring fluorescence. The gap in the record begins at the flash onset (arrow) and lasts 1·7 ms. Ca^{2+} rose from 113 nM to levels which nearly saturated fluo-3, and fell with a τ of 15 ms to a steady-state level of 238 nM (average of ten records). *B*, absence of a Ca^{2+} spike after photolysis in neurons (intracellular). This record represents the average fluorescence signal from twenty-nine flashes (three cells) using the same DM–Ca^{2+} solution and identical brief flash. *C*, absence of an intracellular Ca^{2+} spike under standard conditions. This record represents average intracellular Ca^{2+} measured in nine cells using standard duration 100 V flashes and 10 μM fluo-3. The gap due to the flash is 5 ms. Though intracellular Ca^{2+} was raised slightly after these flashes (indicating partial photolysis of DM-nitrophen) no Ca^{2+} spike was detected.

that of Fig. 10*A*, except that this experiment is intracellular. Only a small increase in intracellular Ca^{2+} is seen with no sign of a Ca^{2+} spike. Likewise, the fluo-3 signals recorded following 100 V flashes of the standard duration (see Fig. 2*A*) reveal no fast Ca^{2+} spike, although here recording is not possible until 5 ms following the flash (Fig. 10*C*). The Ca^{2+} spike shown for droplets of DM–Ca^{2+} solution in Fig. 10*A* does not occur in cells (Fig. 10*B* and *C*).

The second argument against the existence of a large, fast spike in intracellular Ca^{2+} is that addition of dibromo-BAPTA to DM–Ca^{2+} solution does not greatly reduce the block of Ba^{2+} current by photolysis. Addition of 1 mM dibromo-BAPTA to the DM–Ca^{2+} solution reduces the Ba^{2+} current block (maximal intensity flashes) from 52 ± 19 to 32 ± 14% ($n = 8$ for both conditions, see Fig. 11*B*). Dibromo-BAPTA has a relatively low affinity for Ca^{2+} ($K_d = 1{\cdot}6$ μM) but binds Ca^{2+} rapidly ($K_f = 8 \times 10^8$ M^{-1} s^{-1} for difluoro-BAPTA; Smith, Hesketh, Metcalfe, Feeney & Morris, 1983). Our kinetic model of Ca^{2+} photo-release and buffering (see Methods) suggests that dibromo-BAPTA buffers Ca^{2+} as rapidly as it is released from photolysed DM-nitrophen. Thus, dibromo-BAPTA would greatly suppress any Ca^{2+} spike rising

above 500 nM, while only slightly reducing concentrations below 100 nM. Figure 11*A* illustrates this action of dibromo-BAPTA on the Ca^{2+} spike recorded in a droplet (shown before in Fig. 10*A*). The addition of 1 mM dibromo-BAPTA to the DM–Ca^{2+} solution eliminates the large Ca^{2+} spike immediately following the flash, but only

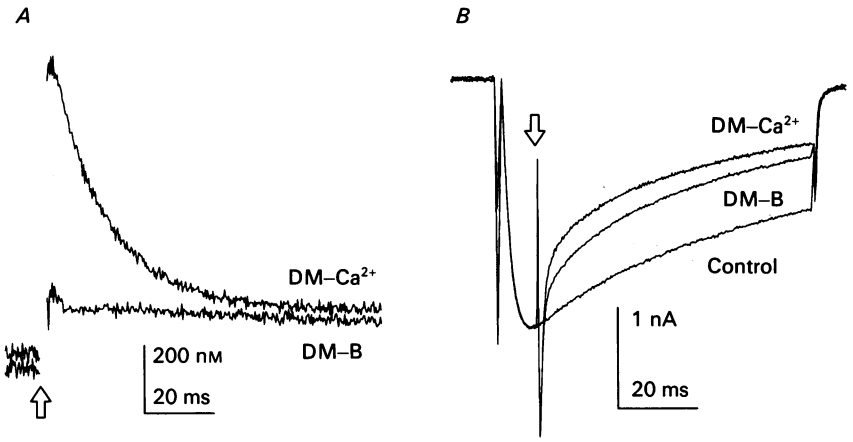

Fig. 11. Effect of dibromo-BAPTA on Ca^{2+} release and Ba^{2+} current block. *A*, addition of 1 mM dibromo-BAPTA to DM–Ca^{2+} solution (DM–B) strongly attenuates the Ca^{2+} spike measured in droplets of DM–Ca^{2+} solution while only slightly reducing steady-state levels (each trace is an average of ten records). The pre-flash Ca^{2+} levels were 113 nM (DM–Ca^{2+}) and 71 nM (DM–B). DM–Ca^{2+} data are the same as in Fig. 10*A*. *B*, Ba^{2+} current blocked after maximal intensity flashes is not greatly reduced by addition of dibromo-BAPTA. Peak currents (before flash) have been superimposed to allow comparison of the block in each condition (current scale applies to currents with DM–Ca^{2+} solution). Currents shown are averages from eight cells. Arrows indicate flash onset.

slightly reduces the steady-state levels of Ca^{2+}. If most of the Ba^{2+} current block were occurring due to an intracellular Ca^{2+} spike during the first few milliseconds after the flash, dibromo-BAPTA should almost completely eliminate the block of Ba^{2+} current. The small effect of dibromo-BAPTA on Ba^{2+} current block (Fig. 11*B*) suggests that endogenous buffers can take up photo-released Ca^{2+} almost as fast as dibromo-BAPTA, which is fast enough to keep up with the Ca^{2+} photo-release in this study.

Concentration dependence of Ca^{2+} block

The amount of Ba^{2+} current blocked by photo-released Ca^{2+} increases with the intensity of the flash. Figure 12*A* shows the results of an experiment in which flashes of each intensity are applied to one cell; the onset of flashes is indicated by the arrow. Flashes are separated by at least 7 min and applied in various orders of intensity so that the average block will not be systematically influenced by possible irreversible effects of flashes. In Fig. 12*B*, the average block (n = 8–16) is plotted against the average peak intracellular Ca^{2+} concentration measured for each flash intensity. Since Ba^{2+} current is blocked by even the smallest jump in intracellular Ca^{2+}, it appears that some fraction is already blocked by the steady-state level of Ca^{2+}

(36 nM). This conclusion is supported by our observation that the average Ba^{2+} current was 10% larger in those cells dialysed with DM–EGTA solution and 26% larger when dibromo-BAPTA was added to DM–Ca^{2+} solution. Both of these solutions should yield a lower intracellular Ca^{2+} concentration than DM–Ca^{2+}

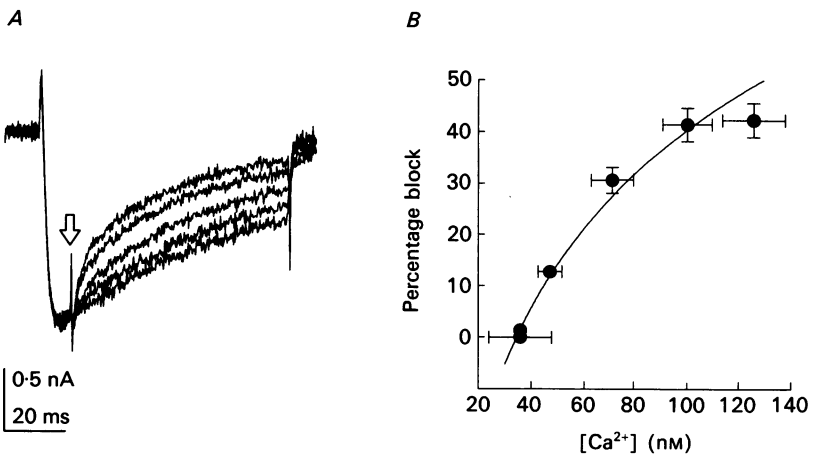

Fig. 12. Dependence of block on intracellular Ca^{2+}. Ba^{2+} current block was measured after flashes of each intensity. *A*, example of current records from one cell showing block after flashes (onset at arrow) ranging from the lowest intensity (largest inward current at the end of the pulse), to the highest (smallest inward current). Flashes were separated by at least 7 min. *B*, percentage block (±standard error, $n = 8$–16) of peak Ba^{2+} current *versus* $[Ca^{2+}]_i$ measured as early as possible after flashes (from Fig. 9*A*). In half of the cells, block was measured at the end of the pulse and corrected to give the expected block of peak Ba^{2+} current. The continuous line represents the predicted relation with a K_d of 50 nM (see Discussion).

solution alone. The smooth line in Fig. 12*B* indicates the concentration dependence of block assumed in our simple model (see Discussion). Given the uncertainty in each measure (block and Ca^{2+}), the data agree reasonably well with this curve. There is some suggestion in the data that the block might saturate at a value less than 100%, as though some fraction of Ba^{2+} current were insensitive to intracellular Ca^{2+}.

DISCUSSION

Intracellular Ca^{2+} after flash photolysis of DM-nitrophen

In an ideal study of Ca^{2+} channel block by intracellular Ca^{2+}, step changes in intracellular Ca^{2+} would be made. Caged Ca^{2+} compounds can produce a rapid, spatially uniform release of Ca^{2+}, but in general do not create a step increase in intracellular Ca^{2+}. Subsequent uptake of the released Ca^{2+} by either unphotolysed caged Ca^{2+} compound (Grell *et al.* 1989) or by molecules endogenous to the cell shape the Ca^{2+} signal. Even the loading of the Ca^{2+} cage is not controlled by the experimenter since a healthy cell will bring the level of intracellular Ca^{2+} toward some intrinsic set point. In these experiments, cells dialysed with DM–Ca^{2+} solution, which had 113 nM Ca^{2+}, were found to have only 36 nM Ca^{2+}. At this low Ca^{2+}

concentration, nitr-5, another Ca^{2+} cage with both a lower affinity for Ca^{2+} (145 nM compared to 5 nM) and a lower quantum efficiency, is insufficiently loaded to significantly increase intracellular Ca^{2+} after the maximal intensity flashes we applied in this study. Preliminary experiments confirmed this limitation. Due to the

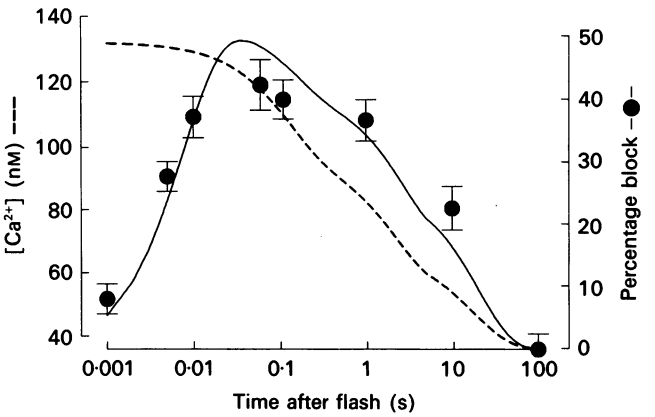

Fig. 13. Time course of Ca^{2+} channel block and recovery fitted with a simple model. Ba^{2+} current block (●) and intracellular Ca^{2+} (dashed line) measured after maximal intensity flashes are summarized on this logarithmic time scale. Both block at 1 ms and intracellular Ca^{2+} before 20 ms were extrapolated from the data presented in previous figures. The continuous line represents the predicted time course of block from a simple two-state model (open and blocked channels), using a K_d of 50 nM and forward rate constant of 7×10^8 M^{-1} s^{-1}.

cell's ability to maintain Ca^{2+} homeostasis, experiments involving Ca^{2+} photo-release are difficult to interpret unless intracellular Ca^{2+} is measured directly.

The dashed line in Fig. 13 represents the Ca^{2+} transient measured in *Lymnaea* neurons following a maximal UV flash. Measurements were made from 20 ms to 10 min after the flash using the fluorescent indicator fluo-3, fitted with three exponentials (120 ms, 2 and 13 s), and shown here on a logarithmic time scale. Intracellular Ca^{2+} was not measured during the first 20 ms due to PMT saturation by the flash. The Ca^{2+} concentration measured immediately after the flash is only one-hundredth of the level expected given the reduced Ca^{2+} loading of DM-nitrophen in the cell (Fig. 9*A*). Our interpretation of this result is that endogenous buffers are capable of binding 99% of the photo-released Ca^{2+} in less than 20 ms. Molluscan cell bodies have been shown to have strong Ca^{2+} buffers with K_d values of less than 1 μM (Connor & Ahmed, 1984). In experiments designed to resolve the time course of Ca^{2+} binding to endogenous buffers (Fig. 10*B* and *C*), the duration of any possible rapid intracellular Ca^{2+} spike was limited to less than 2 ms. A computer model of photolytic Ca^{2+} release and binding to Ca^{2+} ligands (see Methods) indicated the forward rate constant for Ca^{2+} binding to the endogenous buffer must be greater than 5×10^7 M^{-1} s^{-1} to explain this result. A second result supporting this idea is the relatively small reduction of Ba^{2+} current block when 1 mM dibromo-BAPTA is added to the DM–Ca solution (Fig. 11). If the endogenous buffer can bind Ca^{2+} as fast as dibromo-BAPTA, has an equal or greater affinity (1 μM K_d), and an equal or larger

capacity (1 mM), then the addition of dibromo-BAPTA would not have much effect on block. A similar conclusion has been reached for the Ca^{2+} buffering of frog saccular hair cell cytoplasm, which is as effective as 0·5–2 mM BAPTA in suppressing Ca^{2+} transients (Roberts & Hagedorn, 1992). In addition, forward rate constants of 10^8 M^{-1} s^{-1} for Ca^{2+} binding to intracellular proteins have been determined for troponin and parvalbumin (Robertson, Johnson & Potter, 1981). Therefore, we have assumed in Fig. 13 that no large, fast Ca^{2+} spike occurs during the first few milliseconds and project the measured decay of intracellular Ca^{2+} back to the time of the flash. The return of intracellular Ca^{2+} to the steady-state level of 36 nM requires more than a minute and is presumably due to Ca^{2+} sequestration by the cell and exchange with the patch electrode. The intracellular Ca^{2+} transient produced by photolysis of nitr-5 in fibroblasts followed a similar time course to that measured here (Kao *et al.* 1989).

An observation of surprisingly small increases in fluo-3 fluorescence on photolysis of DM-nitrophen in snail neurons prompted Zucker (1992) to look for interference between DM-nitrophen and the fluorescence of fluo-3. He found that at higher concentrations of fluo-3 (100 μM) and DM-nitrophen (10 mM), fluo-3 fluorescence was quenched when free Ca^{2+} was 1 μM or less. We normally used concentrations of DM-nitrophen and fluo-3 an order of magnitude lower than those at which Zucker discovered this interference. A number of observations suggest that such interference was not a serious complication in our measurements. Fluo-3 Ca^{2+} measurements in DM–Ca^{2+} solution droplets gave a value (113 nM) close to that measured with Ca^{2+}-sensitive electrodes (42 nM) or calculated (51 nM). Ca^{2+} measured with fluo-3 in droplets also fit the predicted flash intensity–Ca^{2+} relation (Fig. 9*A*, ■——■). Our conclusion that neurons have an endogenous buffer that rapidly binds most of the photo-released Ca^{2+} is based on a comparison between the same solution inside and outside cells (droplets), and is thus independent of the interference studied by Zucker. A similar interference between either fluo-3 or DM-nitrophen and cytoplasm, however, remains a possibility.

Ca^{2+} sensitivity of Ca^{2+} channels

There is considerable disagreement in the literature as to the levels of intracellular Ca^{2+} that block Ca^{2+} channels. In agreement with the results reported here, several previous studies have found that Ca^{2+} currents are sensitive to intracellular Ca^{2+} as low as 100 nM. Hagiwara & Nakajima (1966) found that the all-or-none Ca^{2+} spikes of barnacle muscle changed to graded responses when intracellular Ca^{2+} was raised above 80 nM, and that all active responses were eliminated above 500 nM. Plant *et al.* (1983) measured the resting concentration of intracellular Ca^{2+} in *Helix* neurons to be 190 nM using a Ca^{2+}-sensitive microelectrode. Injection of buffered Ca^{2+} solutions with less than 180 nM free Ca^{2+} increased the magnitude of the Ca^{2+} current, while solutions greater than 890 nM decreased the Ca^{2+} current. Ca^{2+} current of rabbit vein smooth muscle was also blocked with a K_d of about 100 nM (Ohya, Kitamura & Kuriyama, 1988). Previous studies on *Lymnaea* neurons concluded that raising intracellular Ca^{2+} to 1 μM completely blocked the Ca^{2+} current (Byerly & Moody, 1984). On the other hand, a recent study of identified *Helix* neurons found that injected solutions with less than 500 nM Ca^{2+} had little or no effect on the peak Ca^{2+} current, while higher concentrations reduced the Ca^{2+} current (Gutnick, Lux,

Swandulla & Zucker, 1989). When L-type Ca^{2+} channels are studied in inside-out patches or planar bilayers in the presence of the agonist Bay K 8644, the channels are only sensitive to millimolar concentrations of Ca^{2+}. The measured K_d for block by intracellular Ca^{2+} was 4 mM for cardiac Ca^{2+} channels (Rosenberg *et al.* 1988) and 5·8 mM for smooth muscle Ca^{2+} channels (Huang *et al.* 1989). It is not clear if the low sensitivity to intracellular Ca^{2+} found in these studies represents a property of these channels under physiological conditions or if it is due to channel isolation or the use of agonist.

The filled circles in Fig. 13 summarize the rapid block of Ca^{2+} channels following a maximal flash (τ of 5 ms) and the subsequent slow recovery of the Ba^{2+} current (τ of 16 s). In similar studies done on dorsal root ganglion neurons, intracellular photo-released Ca^{2+} was found to block Ca^{2+} channels with a time constant of 7 ms (Morad *et al.* 1988). A mean time constant of 18 s was measured for recovery of Ca^{2+} currents in *Helix* neurons following block by injections of Ca^{2+} (Plant *et al.* 1983). This last result represents remarkably good agreement considering that our experiments were performed on internally dialysed cells, while the *Helix* neurons were intact. The continuous line in Fig. 13 shows the time course for block and recovery calculated from the Ca^{2+} time course (dashed line) and a simple first-order model for Ca^{2+} channel block. The forward rate constant for Ca^{2+} binding and channel block was assumed to be 7×10^8 M^{-1} s^{-1} with a K_d of 50 nM. This model implies that 42% of the Ca^{2+} channels are blocked at the pre-flash level of intracellular Ca^{2+} (36 nM). The right-hand ordinate of the plot is given in the same units as are used throughout Results (i.e. the pre-flash level is designated 0% block). Although this simple model slightly overestimates the peak block and predicts a recovery that is somewhat faster than actually observed, it accounts for the block and recovery surprisingly well.

In the simple model discussed above we have assumed that all the Ca^{2+} channels can be blocked by intracellular Ca^{2+}. Although the data of Fig. 12*B* are consistent with this assumption (continuous line in Fig. 12*B*), there is some suggestion in this data that the block might saturate at a value less than 100%. A component of the Ba^{2+} current resistant to raised intracellular Ca^{2+} could result from a number of causes. (1) Some of the Ca^{2+} channels might not see the elevation of intracellular Ca^{2+}, either due to DM-nitrophen not reaching their local environment or to UV light not reaching the DM-nitrophen. We doubt this possibility in our experiments since the isolated cell somas have no processes and we have demonstrated little gradient of Ca^{2+} release across the cell. (2) Intracellular Ca^{2+} might not completely block a channel but only reduce its activity. (3) There might be different types of Ca^{2+} channels, some sensitive to intracellular Ca^{2+} and others insensitive to intracellular Ca^{2+}. This idea is appealing since multiple types of Ca^{2+} channels have been demonstrated in many cell types (McCleskey, Fox, Feldman & Tsien, 1986). Some of these channels show only voltage-dependent inactivation, while others exhibit Ca^{2+}-dependent inactivation (Byerly & Hagiwara, 1988; Yue, Backx & Imredy, 1990). Most cells with Ca^{2+} currents which demonstrate Ca^{2+}-dependent inactivation also have voltage-dependent inactivation (Hadley & Hume, 1987; Campbell, Giles, Hume & Shibata, 1988; Akaike, Tsuda & Oyama, 1988). In one hypothesis, separate types of channels are responsible for the two types of inactivation. According to this hypothesis, we might expect to find a fraction of the Ba^{2+} current insensitive to intracellular Ca^{2+}. We doubt this possibility in *Lymnaea* neurons for several reasons.

Figure 4 demonstrates that the voltage dependence of activation and the inactivation of the Ba^{2+} current surviving block are the same as for the total current. When intracellular Ca^{2+} is raised to micromolar levels by dialysing these neurons with a high-Ca^{2+}, ATP-free solution, all the Ca^{2+} current is eliminated (Byerly & Moody, 1984). This last result also argues against the second possibility, that intracellular Ca^{2+} might reduce but not completely block Ca^{2+} channel opening.

Intracellular Ca^{2+} may also enhance Ca^{2+} channel activity as well as inhibit it. From studies of cardiac Ca^{2+} current, Marban & Tsien (1982) proposed that small increases of intracellular Ca^{2+} might facilitate Ca^{2+} currents while larger increases would block the current. Flash photolysis of nitr-5 in cardiac muscle cells increased the Ba^{2+} current by a factor of more than two (Gurney, Charnet, Pye & Nargeot, 1989). The L-type Ca^{2+} channels of GH_3 cells have also been shown to have longer open times when intracellular Ca^{2+} is increased (Armstrong, Erxleben, Kalman, Lai, Nairn & Greengard, 1988). We found that the Ba^{2+} current was enhanced following recovery from block by photo-released Ca^{2+} in six of sixteen cells (Fig. 6*B*). Such an enhancement was not seen following flashes that did not release Ca^{2+}. Thus, intracellular Ca^{2+} might also promote some processes that facilitate Ca^{2+} channel function in snail neurons.

Site and nature of Ca^{2+} block

The concentration of Ca^{2+} near the inner mouth of the Ca^{2+} channel reaches near millimolar levels within a few microseconds of channel opening (Simon & Llinás, 1985; Neher, 1986). If the block by intracellular Ca^{2+} involves Ca^{2+} binding to a site in the inner mouth of the channel, the slow time course of inactivation could not be due to accumulation of Ca^{2+}, since Ca^{2+} reaches a constant level almost instantly in this region. A slow inactivation could result from a smaller rate constant and lower affinity for Ca^{2+} binding. Sherman *et al.* (1990) propose such a model to describe the Ca^{2+}-dependent inactivation of mouse pancreatic β-cell Ca^{2+} current. Their model assumes an effective dissociation constant of 0·5 mM for the Ca^{2+} binding site and a slow forward rate constant (about 4×10^4 M^{-1} s^{-1}). Clearly, this model is very different from the one we use in Fig. 13. Their model is not tenable for cells in which the Ca^{2+} current is rapidly blocked by submicromolar intracellular Ca^{2+}. However, the intracellular distribution of Ca^{2+} established within microseconds of channel opening limits the location of the high-affinity site in our model. If the site were in the pore of the channel, Ca^{2+} channels would inactivate almost immediately upon opening. Thus, we must assume that this site is located at some distance from the pore. Given the fast (BAPTA-like) properties of the endogenous buffer suggested by our experiments, the site might only be tens of nanometers away from the pore (see Neher, 1986). Thus the site may still be on the Ca^{2+} channel or a closely associated protein.

Chad & Eckert (1986) have proposed that Ca^{2+}-dependent inactivation of Ca^{2+} channels is due to the action of a Ca^{2+}-activated phosphatase. In their scheme, recovery from inactivation requires phosphorylation by a cAMP-dependent kinase. It is now well established that cAMP-dependent phosphorylation plays a central role in the function of certain L-type Ca^{2+} channels (Hille, 1991). However, no clear evidence for a similar role of cAMP-dependent phosphorylation in *Lymnaea* neurons has been obtained. While ATP is important in maintaining Ca^{2+} channel function,

cAMP or catalytic subunit of cAMP-dependent kinase had no effect on the wash-out of Ca^{2+} current (Byerly & Yazejian, 1986). In addition, the presence of a specific cAMP-dependent kinase inhibitor had no effect on the recovery of Ca^{2+} current from block by intracellular Ca^{2+} (Byerly *et al.* 1988). The very fast block of Ba^{2+} current produced by photo-released Ca^{2+} (Fig. 5) appears incompatible with the action of a diffusible Ca^{2+}-activated phosphatase. The forward rate constant required for this fast block is essentially at the diffusion limit. There is little time available for Ca^{2+} to bind and activate a phosphatase, which then must find the phosphorylated site and cleave the bond. Only a tethered phosphatase present as an intimate part of the channel complex could approach such a rapid rate of dephosphorylation. In a number of preliminary experiments with various phosphatase inhibitors we have found none that show an effect on Ca^{2+}-dependent inactivation.

The block of the *Lymnaea* Ca^{2+} channel by intracellular Ca^{2+} is independent of the state of the channel. The block develops at essentially the same rate when the channels are activated as it does when they are closed (Fig. 5*B*). This result is in conflict with models that assume that Ca^{2+} channel inactivation is primarily voltage dependent, but with rate constants that are sensitive to intracellular Ca^{2+} (Gutnick *et al.* 1989). Such models predict that raising intracellular Ca^{2+} will have little effect on the peak magnitude of the Ca^{2+} channel current, but will increase the rate of inactivation during a depolarization. Such behaviour was seen for L-type Ca^{2+} channels in bilayers; Ba^{2+} current inactivated faster when the concentration of Ca^{2+} on the internal side was 15 μM than when it was 10 nM (Hirschberg, Koplas & Rosenberg, 1990). Dephosphorylation did not appear to be involved in this example of Ca^{2+}-dependent inactivation, since recovery from inactivation occurred even in the absence of Mg^{2+} and ATP. In contrast, *Lymnaea* Ba^{2+} currents inactivated at the same rate when intracellular Ca^{2+} was raised (1 s after flash) as they did at the steady-state Ca^{2+} level (Fig. 4*B*).

The experiments described here do not determine the mechanism of Ca^{2+} channel block by intracellular Ca^{2+}. However, the rapid time course of block measured here limits the possible complexity of the mechanism. The high affinity of the blocking site indicates that even the resting level of intracellular Ca^{2+} will strongly control the activity of Ca^{2+}-sensitive, voltage-dependent Ca^{2+} channels. Since these channels in turn serve as one source for this important second messenger, Ca^{2+} plays an unusually direct role in controlling its own entry into the cell.

We wish to thank Henry Lester for the use of the flash lamp, his helpful advice throughout the project, and comments on the manuscript; George Augustine for introducing us to Ca^{2+} indicators, use of his equipment in early Ca^{2+} indicator experiments, and comments on the manuscript; Ian Parker for advice on the confocal measurement of fluorescence; Tony DeFazio for writing programs used to calculate steady-state Ca^{2+}; and John Walsh for comments on the manuscript. This work was supported by National Institute of Neurological Disorders and Stroke grant NS28484.

REFERENCES

AKAIKE, N., TSUDA, Y. & OYAMA, Y. (1988). Separation of current- and voltage-dependent inactivation of calcium current in frog sensory neuron. *Neuroscience Letters* **84**, 46–50.

ARMSTRONG, D., ERXLEBEN, C., KALMAN, D., LAI, Y., NAIRN, A. & GREENGARD, P. (1988). Intracellular calcium controls the activity of dihydropyridine-sensitive calcium channels through protein phosphorylation and its removal. *Journal of General Physiology* **92**, 10a.

AUGUSTINE, G. J., CHARLTON, M. P. & HORN, R. (1988). Role of calcium-activated potassium channels in transmitter release at the squid giant synapse. *Journal of Physiology* **398**, 149–164.

BREHM, P. & ECKERT, R. (1978). Calcium entry leads to inactivation of calcium channel in *Paramecium*. *Science* **202**, 1203–1206.

BYERLY, L. & HAGIWARA, S. (1988). Calcium channel diversity. In *Calcium and Ion Channel Modulation*, ed. GRINNELL, A. D., ARMSTRONG, D. & JACKSON, M. B., pp. 3–18. Plenum Press, New York.

BYERLY, L., LEUNG, H. T. & YAZEJIAN, B. (1988). Cellular control of calcium currents. *Biomedical Research* **9**, suppl. **2**, 1–9.

BYERLY, L. & MOODY, W. J. (1984). Intracellular calcium ions and calcium currents in perfused neurones of the snail *Lymnaea stagnalis*. *Journal of Physiology* **352**, 637–652.

BYERLY, L. & SUEN, Y. (1989). Characterization of proton currents in neurones of the snail *Lymnaea stagnalis*. *Journal of Physiology* **413**, 75–89.

BYERLY, L. & YAZEJIAN, B. (1986). Intracellular factors for the maintenance of calcium currents in perfused neurones from the snail *Lymnaea stagnalis*. *Journal of Physiology* **370**, 631–650.

CAMPBELL, D. L., GILES, W. R., HUME, J. R. & SHIBATA, E. F. (1988). Inactivation of calcium current in bull-frog atrial myocytes. *Journal of Physiology* **403**, 287–315.

CHAD, J. E. & ECKERT, R. (1986). An enzymatic mechanism for calcium current inactivation in dialysed *Helix* neurones. *Journal of Physiology* **378**, 31–51.

CONNOR, J. A. & AHMED, Z. (1984). Diffusion of ions and indicator dyes in neural cytoplasm. *Cellular and Molecular Neurobiology* **4**, 53–66.

EBERHARD, M. & ERNE, P. (1989). Kinetics of calcium binding to fluo-3 determined by stopped-flow fluorescence. *Biochemistry and Biophysics Research Communications* **163**, 309–314.

ECKERT, R. & CHAD, J. E. (1984). Inactivation of Ca^{2+} channels. *Progress in Biophysics and Molecular Biology* **44**, 215–267.

GRELL, E., LEWITZKI, E., RUF, H., BAMBERG, E., ELLIS-DAVIES, G. C., KAPLAN, J. H. & DEWEER, P. (1989). Caged-Ca^{2+}: a new agent allowing liberation of free Ca^{2+} in biological systems by photolysis. *Cellular and Molecular Biology* **35**, 515–522.

GURNEY, A. M., CHARNET, P., PYE, J. M. & NARGEOT, J. (1989). Augmentation of calcium current by flash photolysis of intracellular caged-Ca^{2+} molecules. *Nature* **341**, 65–68.

GURNEY, A. M., TSIEN, R. Y. & LESTER, H. A. (1987). Activation of a potassium current by rapid photochemically generated step increases of intracellular calcium in rat sympathetic neurons. *Proceedings of the National Academy of Sciences of the USA* **84**, 3496–3500.

GUTNICK, M. J., LUX, H. D., SWANDULLA, D. & ZUCKER, H. (1989). Voltage-dependent and calcium-dependent inactivation of calcium channel current in identified snail neurons. *Journal of Physiology* **412**, 197–220.

HADLEY, R. W. & HUME, J. R. (1987). An intrinsic potential-dependent inactivation mechanism associated with calcium channels in guinea-pig myocytes. *Journal of Physiology* **389**, 205–222.

HAGIWARA, S. & NAKAJIMA, S. (1966). Effects of the intracellular Ca^{2+} ion concentration upon the excitability of the muscle fiber membrane of a barnacle. *Journal of General Physiology* **49**, 807–818.

HILLE, B. (1991). Modulation, slow synaptic action, and second messengers. In *Ionic Channels of Excitable Membranes*, pp. 170–201. Sinauer Associates, MA, USA.

HIRSCHBERG, Y., KOPLAS, P. A. & ROSENBERG, R. L. (1990). Calcium and calcineurin increase the inactivation rate of L-type calcium currents in planar bilayers. *Society for Neuroscience Abstracts* **16**, 1174.

HUANG, Y., QUALE, J. M., WORLEY, J. F., STANDEN, N. B. & NELSON, M. T. (1989). External cadmium and internal calcium block of single calcium channels in smooth muscle cells from rabbit mesenteric artery. *Biophysical Journal* **56**, 1023–1028.

JOHNSON, B. D. & BYERLY, L. (1991*a*). Calcium channel block by photo-released intracellular calcium. *Society for Neuroscience Abstracts* **17**, 901.

JOHNSON, B. D. & BYERLY, L. (1991*b*). Control of neuronal calcium current by intracellular calcium. *Biomedical Research* **12**, suppl. 2, 49–52.

KAO, J. P., HAROOTUNIAN, A. T. & TSIEN, R. Y. (1989). Photochemically generated cytosolic calcium pulses and their detection by fluo-3. *Journal of Biological Chemistry* **264**, 8179–8184.

KAPLAN, J. H. & ELLIS-DAVIES, G. C. (1988). Photolabile chelators for the rapid photorelease of divalent cations. *Proceedings of the National Academy of Sciences of the USA* **85**, 6571–6575.

KOSTYUK, P. G. & KRISHTAL, O. A. (1977). Effects of calcium and calcium-chelating agents on the inward and outward current in the membrane of mollusc neurones. *Journal of Physiology* **270**, 569–580.

LEE, K. S., MARBAN, E. & TSIEN, R. W. (1985). Inactivation of calcium channels in mammalian heart cells: joint dependence on membrane potential and intracellular calcium. *Journal of Physiology* **364**, 395–411.

MCCLESKEY, E. W., FOX, A. P., FELDMAN, D. & TSIEN, R. W. (1986). Different types of calcium channels. *Journal of Experimental Biology* **124**, 177–190.

MARBAN, E. & TSIEN, R. W. (1982). Enhancement of calcium current during digitalis inotropy in mammalian heart: positive feed-back regulation by intracellular calcium? *Journal of Physiology* **329**, 589–614.

MARTELL, A. E. & SMITH, R. M. (1974). *Critical Stability Constants*, vol. I, Plenum Press, New York.

MORAD, M., DAVIES, N. W., KAPLAN, J. H. & LUX, H. D. (1988). Inactivation and block of calcium channels by photo-released Ca^{2+} in dorsal root ganglion neurons. *Science* **241**, 842–844.

NEHER, E. (1986). Concentration profiles of intracellular calcium in the presence of a diffusible chelator. *Experimental Brain Research* **14**, 80–96.

OHYA, Y., KITAMURA, K. & KURIYAMA, H. (1988). Regulation of calcium current by intracellular calcium in smooth muscle cells of rabbit portal vein. *Circulation Research* **62**, 375–383.

PLANT, T. D., STANDEN, N. B. & WARD, T. A. (1983). The effects of injection and calcium ions and calcium chelators on calcium channel inactivation in *Helix* neurones. *Journal of Physiology* **334**, 189–212.

RAPP, G. & GÜTH, K. (1988). A low cost high intensity flash device for photolysis experiments. *Pflügers Archiv* **411**, 200–203.

ROBERTS, W. M. & HAGEDORN, M. (1992). Cytoplasm of frog saccular cells has a calcium buffer more effective than 0·5 mM BAPTA. *Biophysical Journal* **61**, A142.

ROBERTSON, S. P., JOHNSON, J. D. & POTTER, J. D. (1981). The time-course of Ca^{2+} exchange with calmodulin, troponin, parvalbumin, and myosin in response to transient increases in Ca^{2+}. *Biophysical Journal* **34**, 559–569.

ROSENBERG, R. L., HESS, P. & TSIEN, R. W. (1988). Cardiac calcium channels in planar lipid bilayers. L-type channels and calcium-permeable channels open at negative membrane potentials. *Journal of General Physiology* **92**, 27–54.

SALA, F. & HERNANDEZ-CRUZ, A. (1990). Calcium diffusion modeling in a spherical neuron: relevance of buffering properties. *Biophysical Journal* **57**, 313–324.

SHERMAN, A., KEIZER, J. & RINZEL, J. (1990). Domain model for Ca^{2+}-inactivation of Ca^{2+} channels at low channel density. *Biophysical Journal* **58**, 985–995.

SIMON, S. M. & LLINÁS, R. R. (1985). Compartmentalization of the submembrane calcium activity during calcium influx and its significance in transmitter release. *Biophysical Journal* **48**, 485–498.

SMITH, G. A., HESKETH, R. T., METCALFE, J. C., FEENEY, J. & MORRIS, P. G. (1983). Intracellular calcium measurements by ^{19}F NMR of fluorine-labeled chelators. *Proceedings of the National Academy of Sciences of the USA* **80**, 7178–7182.

TILLOTSON, D. (1979). Inactivation of Ca^{2+} conductance dependent on entry of Ca^{2+} ions in molluscan neurons. *Proceedings of the National Academy of Sciences of the USA* **76**, 1497–1500.

TSIEN, R. Y. & RINK, T. J. (1980). Neutral carrier ion-selective microelectrode for measurement of intracellular free calcium. *Biochimica et Biophysica Acta* **599**, 623–638.

YUE, D. T., BACKX, P. H. & IMREDY, J. P. (1990). Calcium-sensitive inactivation in the gating of single calcium channels. *Science* **250**, 1735–1738.

ZUCKER, R. S. (1992). Effects of photolabile calcium chelators on fluorescent calcium indicators. *Cell Calcium* **13**, 29–40.